Neurocomputing 423 (2021) 506–517

Contents lists available at ScienceDirect

Neurocomputing

journal homepage: www.elsevier.com/locate/neucom

Observer-based adaptive fixed-time formation control for multi-agent systems with unknown uncertainties

Tianyi Xiong, Zhou Gu *

College of Mechanical and Electronic Engineering, Nanjing Forestry University, Nanjing 210037, China

ARTICLE INFO

Article history:
Received 4 January 2020
Revised 18 August 2020
Accepted 13 October 2020
Available online 5 November 2020
Communicated by Zidong Wang

Keywords:
Fixed time
Formation control
Multi-agent system

ABSTRACT

This paper investigates the fixed-time formation tracking control problem for multi-agent systems with model uncertainties and in absence of leader's velocity measurements. For each follower, a novel fixed-time cascaded leader state observer (FTCLSO) without velocity measurements is first designed to reconstruct the states of the leader. Then, radial basis function neural networks (RBFNNs) are adopted to approximate the model uncertainties online. Based on the proposed FTCLSO and RBFNNs, a novel fixed-time formation control scheme is constructed to address the time-varying formation tracking problem by utilizing fixed-time nonsmooth backstepping technique. The fixed-time convergence of the formation tracking error is guaranteed through Lyapunov stability analysis. Finally, simulation results demonstrate the effectiveness of the proposed formation tracking control scheme.

1. Introduction

Cooperative control for multi-agent systems has received considerable attention and achieved abundant accomplishments in the recent decades from various scientific communities [1,2]. One of the most significant and fundamental issues of cooperative control is the formation control problem. Three typical control frameworks, namely leader–follower based [3], virtual structure based [4], and behaviour based strategies [5], have been widely investigated and applied in formation control. However, all these three frameworks have their own drawbacks [6]. The leader–follower based strategies may be lack of robustness, the virtual structure based methods may lead to a heavy burden on computations and communications, while the behaviour based approaches may encounter challenges of the system stability. Since consensus control strategies possess strong robustness and high flexibility due to full distribution property, increasing research-ers extend consensus theory to formation control, and numerous results have been derived [7–13]. Notice that most of the existing results of formation control are to achieve time-invariant formation. However, such formation shape may limit application scope since the agents need to transform the formation shape to avoid obstacles and deal with other emergencies. Therefore, time-varying formation control has come to the fore, and growing results on time-varying formation control have been conducted in recent years [2,9–12].

It is well known that settling time is a vital performance specification for the formation control problem of multi-agent systems as fast convergence rate exhibits better flexibility and stronger robustness when the systems encounter obstacles, topology transformations, and other complex environments [14]. Comparing to asymptotic convergence, finite-time convergence can pursue the convergence rate effectively. As an extension of finite-time stability, fixed-time stability guarantees that the settling time function derived from stability analysis is independent of initial conditions and uniformly bounded, while the settling time of finite-time stability grows unbounded along with the value of the initial states [15]. Fixed-time stability is first proposed in [16]. Then it is applied in the fixed-time consensus control for multi-agent systems in [17]. As a result, fruitful results of fixed-time cooperative consensus and formation control for multi-agent systems emerge [18–25]. For first-order multi-agent systems with external disturbances, a robust fixed-time consensus control law with directed topology is proposed in [19]. For second-order multi-agent systems, nonsingular fixed-time consensus control protocols are designed in [20,21]. For high-order multi-agent systems, a novel cascade control structure based on a fixed-time distributed observer is constructed in [22]. For multi-robot systems, the fixed-time formation tracking problem under nonholonomic contraints is investigated in [23]. For multiple autonomous underwater vehicle systems, a compensator-based command filtered fixed-time formation control algorithm with event-triggered communication strategy is proposed in [24].

* Corresponding author.
E-mail address: gzh1808@163.com (Z. Gu).

https://doi.org/10.1016/j.neucom.2020.10.074
0925-2312/

It is worth noting that the majority of the existing fixed-time formation/ consensus control methods, including the aforementioned results, are heavily dependent on the accurate states including position and velocity states of the leader. Nevertheless, in some situations, for instance, when utilizing UWB location technology, it is relatively easier to obtain precise position information comparing to getting accurate velocity measurements for the velocity measurements may be contaminated by noises in practical. It is no doubt that inaccurate velocity measurements of the leader can lead to the deterioration of the formation control performance [26]. For the sake of solving the above problem, the researches based on velocity observers are investigated in [26,27]. Furthermore, as a matter of fact, only the followers having the direct link to the leader can receive the state information of the leader due to the distributed control property, which increases the difficulty of control design and analysis. Therefore, to simplify the control design, a great deal of results on distributed observers to reconstruct the states of the leader are obtained in [22,28,29], such that each follower can obtain the estimates of the leader's states. It should be pointed out that the majority of the existing observers are asymptotically stable or finite-time stable. Actually, the settling time of the observers is also of great significance to the formation control performance. In the works of [22,30], high-order distributed fixed-time observers under connected topologies and a directed graph having a spanning tree are designed. However, both the position and velocity measurements of the leader are required. Unfortunately, it is nontrivial to directly extend the results in [22,30] to the ones without velocity measurements of the leader. The difficulty arises from the complexity of the fixed-time convergence analysis.

For multi-agent system formation control design, another important issue is how to work with the uncertainties. To deal with them, neural network (NN), which can be regarded as a universal approximator, is usually applied in consensus formation control to approximate the unknown uncertainties [31–34]. Based on radial basis function neural networks (RBFNNs) and a disturbance observer, the event-triggered consensus tracking control problem for multi-agent systems with unknown uncertainties and external disturban-ces is investigated in [33]. For a class of nonaffine nonlinear multi-agent systems, a NN-based adaptive consensus protocol is developed to deal with the control difficulty caused by the nonaffine dynamics in [34]. However, the tracking errors under the above control strategies are only uniformly ultimately bounded (UUB). For a class of uncertain nonlinear systems, a fixed-time adaptive control strategy based on NNs is proposed in [35]. Nevertheless, it is assumed that the norm of the weight error matrix $\tilde{\theta}_j$ is bounded beforehand, which is really critical in practical. In the work of [36], fixed-time consensus is acquired for multi-agent systems with nonlinear uncertainties. However, the uncertainty function needs to satisfy Lipschitz continuity condition. Similar condition also appears in [36–38]. Furthermore, the entire accurate states measurements of the leader are indispensable to stabilize the system in the above results. Such necessary conditions limit the applications of the formation control systems in a great extend.

It is well known that backstepping technique is effective in nonlinear systems with uncertainties. However, traditional backstepping technique suffers from "explosion of complexity" caused by the repeated derivations of virtual control inputs. To deal with this problem, dynamic surface control and command filtered backstepping control are proposed in [39–41]. In spite of these achievements, the filtering errors based on the aforementioned backstepping techniques are merely convergent asymptotically rather than in fixed time. To the best of our knowledge, the fixed-time adaptive formation control design without velocity measurements utilizing backstepping technique in presence of uncertainties is still an open problem.

Motivated by the above observations, in this paper, we propose a novel adaptive fixed-time formation tracking control scheme for multi-agent systems based on fixed-time cascaded leader state observer (FTCLSO) without velocity measurements of the leader. Firstly, a novel FTCLSO is designed such that each follower can get the estimates of the leader's states without velocity measurements in fixed time. Secondly, RBFNNs are utilized to approximate the unknown model uncertainties. Finally, an adaptive fixed-time formation control scheme with the designed FTCLSO and RBFNNs based on nonsmooth backstepping technique is constructed to address the time-varying formation tracking control problem in presence of uncertainties and in absence of leader's velocity measurements. The fixed-time convergence of the formation tracking error is obtained through Lyapunov approach, and the simulation results verify the effectiveness of the developed control scheme.

Compared with the previous relevant results, the outstanding features of the control scheme proposed in this paper can be summarized as follows.

(1) Different from the existing leader's states observers in [21,22,26,27,30,42–44], the novel FTCLSO proposed in this paper can not only operate well without velocity measurements of the leader, but also reconstruct the states of the leader for each follower in fixed-time.
(2) The proposed formation control scheme for multi-agent systems based on RBFNN and FTCLSO without velocity measurements can achieve the fixed-time convergence of the formation tracking error in presence of the unknown uncertainties. Strict stability analysis is given, and the simulation results verify the validity and effectiveness of the formation control scheme. In comparison with the works in [31–34], the fixed-time formation control scheme based on RBFNN and FTCLSO achieves that the formation tracking errors converge to a small region around the origin in fixed-time rather than UUB. Compared to the results in [35,44], the proposed formation control scheme can operate well in absence of the velocity measurements of the leader. Therefore, the proposed control scheme is really novel and practical. The simultaneous existences of the leader state observation errors, the RBFNN approximation errors and the filtering errors increase the difficulty of the control scheme design and stability analysis.
(3) The nonsmooth backstepping technique with the fixed-time filter is developed. Compared to the traditional backstepping technique, the proposed nonsmooth backstepping technique can not only deal with the problems of singularity and "explosion of complexity", but also guarantee the fixed-time convergence of the filtering error. In addition, the proposed fixed-time formation control scheme for the multi-agent systems can achieve time-varying formation tracking, which can cope with more complicated tasks compared to time-invariant formation.

The rest of the paper is organized as follows. The preliminaries are introduced in Section 2. Formation control problem description is given in Section 3. The time-varying formation tracking control scheme design and analysis are studied in Section 4. Numerical simulation results are presented in Section 5, after which the conclusions are drawn.

2. Preliminaries

In this section, some useful definitions and lemmas on fixed-time stability and graph theory will be firstly introduced, which play a vital role to obtain the main results of this paper. Then, the notations are presented for the readability of this paper.

2.1. Fixed-time stability

Consider the following system

$$\dot{x}(t) = f(t,x), x(t_0) = x_0, \tag{1}$$

where $x(t) \in R^n$ and $f(t,x) : R^{n+1} \to R^n$ is a nonlinear function vector. Suppose the origin is an equilibrium point of system (1).

Definition 1. [22] The origin of system (1) is said to be globally finite-time stable if it is globally asymptotically stable and the solution $x(t,x_0)$ of system (1) reaches the origin at some finite moment, i.e., $x(t,x_0) = 0, t \leqslant T(x_0)$, where $T : R^n \to R_+ \cup \{0\}$ is the settling time function.

Definition 2. [16] The origin of system (1) is said to be globally fixed-time stable if it is globally finite-time stable and the settling time $T(x_0)$ is globally bounded, i.e., there exists a finite constant $T_M > 0$, such that $T(x_0) \leqslant T_M$ and $x(t) = 0$, $\forall x_0 \in R^n$, and $t \geqslant T_M$.

The following lemmas give the sufficient condition of fixed-time stability of system (1).

Lemma 1 (*[15,16]*). *If there exists a continuous radially unbounded and positive definite function $V(x)$ such that*

$$\dot{V}(x) \leqslant -k_1 V^p(x) - k_2 V^q(x), \tag{2}$$

where $k_1, k_2 > 0, p > 1, 0 < q < 1$. Then the origin of system (1) is globally fixed-time stable and the settling time function T can be estimated by

$$T \leqslant T_{Max} := \tfrac{1}{k_1(p-1)} + \tfrac{1}{k_2(1-q)}. \tag{3}$$

Lemma 2 (*[35,45]*). *If there exists a continuous radially unbounded and positive definite function $V(x)$ such that*

$$\dot{V}(x) \leqslant -k_1 V^p(x) - k_2 V^q(x) + \eta_0, \tag{4}$$

where $k_1, k_2 > 0, p > 1, 0 < q < 1, \eta_0 > 0$. Then the origin of system (1) is practical fixed-time stable and the settling time function T can be estimated by

$$T \leqslant T_{Max} := \frac{1}{k_1\bar{\phi}(p-1)} + \frac{1}{k_2\bar{\phi}(1-q)}, \tag{5}$$

where $0 < \bar{\phi} < 1$. The residual set of the solution of system (1) is given by

$$x \in \left\{ x | V(x) \leqslant \min\left\{ \left(\frac{\eta_0}{(1-\bar{\phi})k_1}\right)^{\frac{1}{p}}, \left(\frac{\eta_0}{(1-\bar{\phi})k_2}\right)^{\frac{1}{q}} \right\} \right\}. \tag{6}$$

The following lemmas are also significant for the stability analysis.

Lemma 3 [20]. *Let $\imath_1, \imath_2, \ldots, \imath_n \geqslant 0$ and $0 < p \leqslant 1$. Then,*

$$\sum_{i=1}^{n} \imath_i^p \geqslant \left(\sum_{i=1}^{N} \imath_i\right)^p. \tag{7}$$

Lemma 4 [30]. *Let $\imath_1, \imath_2, \ldots, \imath_n \geqslant 0$ and $q > 1$. Then,*

$$n^{(1-q)}\left(\sum_{i=1}^{n} \imath_i\right)^q \leqslant \sum_{i=1}^{n} \imath_i^q \leqslant \left(\sum_{i=1}^{n} \imath_i\right)^q. \tag{8}$$

2.2. Basic concepts on graph theory

Consider a multi-agent system comprising Nfollowers and one leader. Generally, we invoke a graph denoted by $G = (V, E, A)$ to describe the information exchanges among the followers. Denote a single follower as node υ_i . Then $V = \{\upsilon_1, \upsilon_2, \ldots, \upsilon_N\}$ is the set of the followers, and $E \subseteq V \times V$ represents the set of edges, where $E$is defined such that if $(\upsilon_j, \upsilon_i) \in E, j \neq i$, there is an edge from follower $j$to the follower i, which means that follower $j$can deliver information to follower i. In addition, matrix $A = [a_{ij}] \in R^{N\times N}$ is the associated adjacency matrix with $a_{ij} \geqslant 0$. We set $a_{ij} > 0, j \neq i$ if and only if $(\upsilon_j, \upsilon_i) \in E$; otherwise $a_{ij} = 0$. In this case, follower $j$is said to be the neighbour of follower $i$if and only if $a_{ij} > 0$. $N_i = \{\upsilon_j \in V : (\upsilon_j, \upsilon_i) \in E\}$ represents the neighbour set of the ith follower. A graph is an undirected graph if and only if $a_{ij} = a_{ji}$. Define $D = \mathrm{diag}\{\chi_1, \chi_2, \ldots, \chi_N\}$ as the in-degree matrix, where $\chi_i = \sum_{\upsilon_j \in N_i} a_{ij}$. Then, the Laplacian matrix of graph $L$is defined as $L = D - A$. A direct path from follower $i$to $j$is a sequence of successive edges in the form of $\{(\upsilon_i, \upsilon_k), (\upsilon_k, \upsilon_l), \ldots, (\upsilon_m, \upsilon_j)\}$. Furthermore, an undirected graph is called connected if there is a path between any two followers in the graph. In the leader–follower case, the element of the adjacency matrix associated with the edge from the ith follower to the leader is denoted by $b_i \geqslant 0$. $b_i > 0$ if and only if the ith follower can receive the state information from the leader; otherwise $b_i = 0$.

In this paper, we suppose the following assumption naturally holds.

Assumption 1. The graph Gamong the followers is connected, and at least one follower can receive the state information from the leader.

2.3. Notations

Throughout this paper, the following notations are used. I_n represents $n$dimensional identity matrix; 1_n stands for $n$dimensional vector with all elements being 1. For real number $\alpha, |\alpha|$ is the absolute value of α ; for any vector $X = [x_1, x_2, \ldots, x_n]^T \in R^n$, $|X| = [|x_1|, |x_2|, \ldots, |x_n|]^T$; for vector $Y = [Y_1, Y_2, \ldots, Y_n]^T$ and $Z = [Z_1, Z_2, \ldots, Z_n]^T, |Y| > |Z|$ means $|Y_i| > |Z_i|, \forall i = 1, 2, \ldots, n$; $|Y| \leqslant |Z|$ means $|Y_i| \leqslant |Z_i|, \forall i = 1, 2, \ldots, n$. $\|X\|_p$ with $p \geqslant 1$ denotes the p-norm of the vector X; $\|A\|_F$ is the Frobenius norm of matrix A; $\sigma_{\max}$ and $\sigma_{\min}$ are the maximum and minimum singular values of matrix A, respectively. $\otimes$ denotes the Kronecker product. For any real number $x \in R$ and any non-negative real number α , function $\lceil x \rfloor^\alpha$ is defined as $\lceil x \rfloor^\alpha = |x|^\alpha \mathrm{sign}(x)$, where $\mathrm{sign}(x)$ represents the signum function of x. For any vector $X = [x_1, x_2, \ldots, x_n]^T$, $\lceil X \rfloor^\alpha = [|x_1|^\alpha \mathrm{sign}(x_1), |x_2|^\alpha \mathrm{sign}(x_2), \ldots, |x_n|^\alpha \mathrm{sign}(x_n)]^T$, $\mathrm{sign}(X) = [\mathrm{sign}(x_1), \mathrm{sign}(x_2), \ldots, \mathrm{sign}(x_n)]^T$. tr(A) represents the trace of matrix A.

3. Problem description

In this paper, we consider a multi-agent system with N followers and one leader. The dynamics of the ith follower can be described as follows:

$$\begin{cases} \dot{x}_i(t) = v_i(t) \\ \dot{v}_i(t) = f_i(x_i(t), v_i(t)) + u_i(t), i = 1, 2, \cdots N, \end{cases} \tag{9}$$

where $x_i(t) \in R^m$ and $v_i(t) \in R^m$ are the position and velocity state vectors of the ith follower with m being the dimension, respectively; $u_i(t) \in R^m$ denotes the control input vector of the ith follower; $f_i(x_i(t), v_i(t)) : R^{2m} \to R^m$ is an unknown but continuous function vector.

Moreover, the dynamics of the leader is described as follows

$$\begin{cases} \dot{x}_0(t) = v_0(t) \\ \dot{v}_0(t) = u_0(t), \end{cases} \tag{10}$$

where $x_0(t) \in R^m$ and $v_0(t) \in R^m$ are position and velocity state vectors of the leader, respectively; $u_0(t) \in R^m$ represents the control input vector of the leader.

In addition, the desired time-varying formation is specified by a command vector $h_i(t) = \left[h_{ix}^T(t), h_{iv}^T(t)\right]^T \in R^{2m}$, where $h_{ix}(t) \in R^m$ and $h_{iv}(t) \in R^m$ are piecewise continuously differentiable function vectors with $\dot{h}_{ix}(t) = h_{iv}(t)$.

Furthermore, the formaiton tracking error vector is defined as $\delta(t) = \left[\delta_{ix}^T(t), \delta_{iv}^T(t)\right]^T \in R^{2m}$, where $\delta_x(t) = \left[\delta_{1x}^T(t), \delta_{2x}^T(t), \ldots, \delta_{Nx}^T(t)\right]^T$ is formation tracking position error vector and $\delta_v(t) = \left[\delta_{1v}^T(t), \delta_{2v}^T(t), \ldots, \delta_{Nv}^T(t)\right]^T$ is formation tracking velocity error vector with $\delta_{ix}(t) = x_i(t) - x_0(t) - h_{ix}(t)$ and $\delta_{iv}(t) = v_i(t) - v_0(t) - h_{iv}(t)$.

To derive the main results of this paper, the following reasonable assumptions are made.

Assumption 2. The control input of the leader $u_0(t)$ is supposed to be unknown. But the norm of $u_0(t)$ is bounded by a positive constant u_M , i.e., $\|u_0(t)\|_\infty \leqslant u_M$, and u_M can be accessible to any follower.

Assumption 3 [46]. The leader's state trajectory at any finite time interval is bounded, i.e., $\|X_0(t)\|_2 \leqslant x_M$ at any finite time interval $[t_0, t]$, where x_M is a positive constant and $X_0 = \left[x_0^T, v_0^T\right]^T$.

Notice that the adaptive NN fixed-time formation control problem by nonsmooth backstepping technique without velocity measurements of the leader still remains unexplored. The control objective of this paper is to design an observer-based adaptive fixed-time formation tracking scheme such that the formation tracking error $\delta(t)$ can converge to a small region around the origin within fixed time, which leads to a successful time-varying formation tracking for the multi-agent system (9) and (10) with unknown uncertainties. For simplicity, we omit (t) for all the variables in the rest of this paper.

4. Formation tracking control scheme design

In this section, a new adaptive fixed-time formation tracking scheme based on FTCLSO and RBFNN, is firstly developed for the multi-agent systems. Then the stability analysis of the closed-loop formation control system is investigated.

4.1. Fixed-time cascaded leader state observer

In this subsection, a novel FTCLSO is designed for each follower to reconstruct the leader's states without velocity measurements of the leader.

For the ith follower, denote $\hat{x}_{0i}$ and $\hat{v}_{0i}$ as the estimates of the leader's states x_0 and v_0 , respectively. Here, we propose the FTCLSO as follows:

$$\begin{cases} \dot{\hat{x}}_{0i} = & \hat{v}_{0i} + \kappa_x \lceil \sum_{v_j \in N_i} a_{ij}(\hat{x}_{0j} - \hat{x}_{0i}) + b_i(x_0 - \hat{x}_{0i}) \rfloor^{q_1} \\ & + \rho_x \mathrm{sign}\left(\sum_{v_j \in N_i} a_{ij}(\hat{x}_{0j} - \hat{x}_{0i}) + b_i(x_0 - \hat{x}_{0i}) \right) \\ \dot{\hat{v}}_{0i} = & \kappa_v \lceil \sum_{v_j \in N_i} a_{ij}(\hat{v}_{0j} - \hat{v}_{0i}) + b_i(z_v - \hat{v}_{0i}) \rfloor^{q_1} \\ & + \rho_v \mathrm{sign}\left(\sum_{v_j \in N_i} a_{ij}(\hat{v}_{0j} - \hat{v}_{0i}) + b_i(z_v - \hat{v}_{0i}) \right), \end{cases} \tag{11}$$

where the observer gains $\kappa_x, \kappa_v, \rho_x, \rho_v > u_M$, the constant $q_1 > 1$. In the case of $b_i > 0, z_v$ is the estimate of v_0 for the followers having the direct communication link to the leader, which can be obtained by the following fixed-time observer:

$$\begin{cases} \dot{z}_x = & z_v - \alpha_1 \lceil (z_x - x_0) \rfloor^{q_2} - \alpha_2 \lceil (z_x - x_0) \rfloor^{\frac{1}{2}} \\ \dot{z}_v = & -\beta \mathrm{sign}(z_x - x_0), z_v(t_0) = v_0(t_0), \end{cases} \tag{12}$$

where z_x is the estimate of x_0 for the followers having the direct communication link to the leader. The observer parameters $q_2 > 1, \alpha_1, \alpha_2, \beta > 0$ satisfy the following condition

$$\begin{cases} \beta > u_M \\ \alpha_2 h^{-1}(\alpha_2) > M, \end{cases} \tag{13}$$

where $M = \beta + u_M, h(\alpha_2) = \frac{1}{\alpha_2} + \left(\frac{2e}{\tilde{m}\alpha_2}\right)^{1/3}$ with $\tilde{m} = \beta - u_M$ and $e$being the base of natural logarithms.

Remark 1. In fact, in the case of $b_i = 0$, that is, for the followers who have no direct communication link to the leader, the fixed-time observer (11) and (12) are both necessary to obtain the estimates of the leader's states in fixed time, while only fixed-time observer (12) is needed for the ith follower satisfying $b_i > 0$. As a whole, fixed-time observers (11) and (12) construct the FTCLSO.

Remark 2. Different from the fixed-time distributed obser-vers in [21,22,30], the FTCLSO consisting of (11) and (12) is only dependent on the position measurements to get the estimates of the leader's states x_0 and v_0 , while the velocity measurements are not necessary. Furthermore, it should be pointed out that the outputs of the observer (12) z_x and z_v can only be acquired by the followers having direct link to the leader, that is, satisfying $b_i > 0$, while the other followers cannot. In addition, if z_x and z_v can be shared between any two followers, the problems of communication link failures clearly make this communication scheme prohibitive. Hence, the online reconstruction of the leader's states without velocity measurements by the FTCLSO within fixed time, is very practical and robust in many applications.

Remark 3. Different from the existing asymptotic and finite-time convergent state observers for multi-agent systems in [26,27,47,48], the proposed FTCLSO can reconstruct the leader's states for each follower in fixed time. As a matter of fact, the convergence rate of the observation error is of great significance to the formation tracking performance of the whole multi-agent system. Fixed-time convergence guarantees that the settling time is irrelevant to initial conditions comparing to finite-time convergence. Thus, the proposed FTCLSO can achieve better formation performance and robustness.

Remark 4. For the ith follower satisfying $b_i > 0$, we may specify $\hat{x}_{0i} = x_{0i}$ and $\hat{v}_{0i} = z_v$ to reduce the burden of computation, while the other followers still employ the reconstructed states $\hat{x}_{0i}$ and $\hat{v}_{0i}$ obtained by the FTCLSO comprising (11) and (12).

Remark 5. Due to the limitation brought by the condition $z_v(t_0) = v_0(t_0)$ in (12), we assume that the leader is static when the followers start to shape a formation and track the trajectory of the leader in this paper, which means the initial velocity of the leader is zero. Thus, it is easy to guarantee that the condition $z_v(t_0) = v_0(t_0)$ is satisfied by setting $z_v(t_0) = 0$. This assumption can hold in many real applications. In the future, we will try our best to extend the obtained results to much more complicated cases, where the followers need to start the formation task when the leader is moving.

Theorem 1. *Suppose Assumptions 1–3 hold. Then the FTCLSO consisting of (11) and (12) can achieve the convergence of the observation errors*

$$\tilde{x}_{0i} = \hat{x}_{0i} - x_{0i} \tag{14}$$

$$\tilde{v}_{0i} = \hat{v}_{0i} - v_{0i} \tag{15}$$

to the origin within fixed time T_0 *, which is bounded by* $T_0 \leqslant T_1 + T_2 + T_3$ *, where*

$$T_1 \leqslant \left(\frac{1}{\alpha_1(q_2-1)\epsilon^{q_2-1}} + \frac{2\epsilon^{1/2}}{\alpha_2}\right)\left(1 + \frac{M\alpha_2}{\bar{m}\alpha_2 - Mh(\alpha_2)}\right), \tag{16}$$

$$T_2 \leqslant \frac{2}{\kappa_v(mN)^{-\frac{1-q_1}{2}}(q_1-1)\Gamma^{\frac{(q_1+1)}{2}}} + \frac{2}{(\rho_v - u_M)\Gamma^{\frac{1}{2}}}, \tag{17}$$

$$T_3 \leqslant \frac{2}{\kappa_x(mN)^{-\frac{1-q_1}{2}}(q_1-1)\Gamma^{\frac{(q_1+1)}{2}}} + \frac{2}{\rho_x\Gamma^{\frac{1}{2}}}. \tag{18}$$

In (16), $\epsilon = (\alpha_2/\alpha_1)^{1/(q_2+1/2)}$ *. In (17) and (18),* $\Gamma = \frac{2\sigma^2_{\min}(H)}{\sigma_{\max}(H)}$ *with* $H = (L + B) \otimes I_m$*.*

Proof. The proof proceeds in three steps. First, we demonstrate that the followers having the direct communication link to the leader can get the estimates of the leader's states in fixed time by the observer (12); then we prove that the observation errors $\tilde{x}_{0i}$ and $\tilde{v}_{0i}$ are bounded at any finite time interval $[t_0, t]$; finally, we show that the observation errors $\tilde{x}_{0i}$ and $\tilde{v}_{0i}$ are able to converge to the origin in fixed time T_0 .

Step 1. Define $\tilde{z}_x = z_x - x_{0i}$ and $\tilde{z}_v = z_v - v_{0i}$. Invoking the dynamics of the leader (10) and the observer (12), the dynamics of $\tilde{z}_x$ and $\tilde{z}_v$ can be written as

$$\begin{cases} \dot{\tilde{z}}_x = \tilde{z}_v - \alpha_1\lceil(\tilde{z}_x)\rfloor^{q_2} - \alpha_2\lceil(\tilde{z}_x)\rfloor^{\frac{1}{2}} \\ \dot{\tilde{z}}_v = -\beta\mathrm{sign}(\tilde{z}_x) - u_0, \tilde{z}_v(t_0) = 0. \end{cases} \tag{19}$$

Then, on the basis of the result in [49], if the observer gains satisfy condition (13), $\tilde{z}_x$ and $\tilde{z}_v$ can uniformly converge to the origin within fixed time T_1 .

Step 2. The dynamics of the observation errors $\tilde{x}_{0i}$ and $\tilde{v}_{0i}$ can be written as follows:

$$\begin{cases} \dot{\tilde{x}}_{0i} = \tilde{v}_{0i} + \kappa_x\lceil\sum_{v_j\in N_i} a_{ij}(\tilde{x}_{0j} - \tilde{x}_{0i}) - b_i\tilde{x}_{0i}\rfloor^{q_1} \\ +\rho_x\mathrm{sign}\left(\sum_{v_j\in N_i} a_{ij}(\tilde{x}_{0j} - \tilde{x}_{0i}) - b_i\tilde{x}_{0i}\right) \\ \dot{\tilde{v}}_{0i} = \kappa_v\lceil\sum_{v_j\in N_i} a_{ij}(\tilde{v}_{0j} - \tilde{v}_{0i}) - b_i\tilde{v}_{0i} + b_i\tilde{z}_v\rfloor^{q_1} - u_0 \\ +\rho_v\mathrm{sign}\left(\sum_{v_j\in N_i} a_{ij}(\tilde{v}_{0j} - \tilde{v}_{0i}) - b_i\tilde{v}_{0i} + b_i\tilde{z}_v\right), \end{cases} \tag{20}$$

Let $\eta_x = [\tilde{x}_{01}^T, \tilde{x}_{02}^T, \ldots, \tilde{x}_{0N}^T]^T$ and $\eta_v = [\tilde{v}_{01}^T, \tilde{v}_{02}^T, \ldots, \tilde{v}_{0N}^T]^T$. Then (20) can be written in a compact form as follows:

$$\begin{cases} \dot{\eta}_x = \eta_v - \kappa_x\lceil H\eta_x\rfloor^{q_1} - \rho_x\mathrm{sign}(H\eta_x) \\ \dot{\eta}_v = -\kappa_v\lceil H\eta_v - \bar{B}(1_N\otimes\tilde{z}_v)\rfloor^{q_1} - \bar{u}_0 - \rho_v\mathrm{sign}(H\eta_v - \bar{B}(1_N\otimes\tilde{z}_v)), \end{cases} \tag{21}$$

where matrix $\bar{B} = B \otimes I_m$, and $\bar{u}_0 = 1_N \otimes u_0$.

Construct the following Lyapunov function:

$$V = V_1 + V_2, \tag{22}$$

where $V_1 = \frac{1}{2}\eta_x^T H\eta_x, V_2 = \frac{1}{2}\eta_v^T H\eta_v$.

Taking the time derivative of V yields

$$\begin{aligned} \dot{V} = \; & -\kappa_x\eta_x^T H\lceil H\eta_x\rfloor^{q_1} - \rho_x\eta_x^T H\mathrm{sign}(H\eta_x) \\ & +\eta_x^T H\eta_v - \kappa_v\eta_v^T H\lceil H\eta_v - \bar{B}(1_N\otimes\tilde{z}_v)\rfloor^{q_1} \\ & -\eta_v^T H\bar{u}_0 - \rho_v\eta_v^T H\mathrm{sign}(H\eta_v - \bar{B}(1_N\otimes\tilde{z}_v)) \\ \leqslant \; & \eta_x^T H\eta_v - \eta_v^T H\bar{u}_0 \\ & -\kappa_v\eta_v^T H\lceil H\eta_v - \bar{B}(1_N\otimes\tilde{z}_v)\rfloor^{q_1} \\ & -\rho_v\eta_v^T H\mathrm{sign}(H\eta_v - \bar{B}(1_N\otimes\tilde{z}_v)) \\ \leqslant \; & \tfrac{1}{2}\eta_x^T H\eta_x + \tfrac{1}{2}\eta_v^T H\eta_v - \eta_v^T H\bar{u}_0 \\ & -\kappa_v\eta_v^T H\lceil H\eta_v - \bar{B}(1_N\otimes\tilde{z}_v)\rfloor^{q_1} \\ & -\rho_v\eta_v^T H\mathrm{sign}(H\eta_v - \bar{B}(1_N\otimes\tilde{z}_v)). \end{aligned} \tag{23}$$

Then the derivative of Vresults in

$$\begin{aligned} \dot{V} \leqslant \; & V - \eta_v^T H\bar{u}_0 \\ & -\kappa_v\eta_v^T H\lceil H\eta_v - \bar{B}(1_N\otimes\tilde{z}_v)\rfloor^{q_1} \\ & -\rho_v\eta_v^T H\mathrm{sign}(H\eta_v - \bar{B}(1_N\otimes\tilde{z}_v)). \end{aligned} \tag{24}$$

To verify the boundedness of the observation errors η_x and η_v in finite time interval $[t_0, t]$, the following three cases are considered:

Case 1. In this case, we assume that the condition $|H\eta_v| > |\bar{B}(1_N\otimes\tilde{z}_v)|$ is satisfied. Then, it is easy to obtain that $\mathrm{sign}(H\eta_v) = \mathrm{sign}(H\eta_v - \bar{B}(1_N\otimes\tilde{z}_v))$. Thus, we have

$$\begin{aligned} \dot{V} \leqslant \; & V - (\rho_v - u_M)\|\eta_v^T H\|_1 \\ \leqslant \; & V. \end{aligned} \tag{25}$$

By solving inequality (25), it is straightforward to get

$$V \leqslant V(t_0)e^{t-t_0}. \tag{26}$$

Case 2. In this case, the condition $|H\eta_v| \leqslant |\bar{B}(1_N\otimes\tilde{z}_v)|$ is considered. From Step 1, $\tilde{z}_v$ can converge to the origin in fixed-time, which follows that $\tilde{z}_v$ is bounded all the time. Hence, there exists a positive constant Ω such that $2^{q_1}\kappa_v\|\bar{B}(1_N\otimes\tilde{z}_v)\|_3^3 + (\rho_v + u_M)\|\bar{B}(1_N\otimes\tilde{z}_v)\|_1 \leqslant \Omega$. Therefore, $\dot{V}$ satisfies

$$\begin{aligned} \dot{V} \leqslant \; & \tfrac{1}{2}\eta_x^T H\eta_x + \tfrac{1}{2}\eta_v^T H\eta_v + 2^{q_1}\rho_v\|\bar{B}(1_N\otimes\tilde{z}_v)\|_3^3 + (\rho_v + u_M)\|\bar{B}(1_N\otimes\tilde{z}_v)\|_1 \\ \leqslant \; & V + \Omega. \end{aligned} \tag{27}$$

Case 3. In this case, consider a general situation, where only a portion of the absolute values of the elements in the vector $|H\eta_v|$ are larger than the corresponding ones in the vector $|\bar{B}(1_N\otimes\tilde{z}_v)|$. Combining the above two cases, it can draw the similar conclusion that

$$\dot{V} \leqslant V + \bar{\Omega}, \tag{28}$$

where $\bar{\Omega} > 0$.

In Cases 2–3, by solving (27) and (28), we can get

$$V \leqslant -\Omega(V(t_0) + \Omega)e^{t-t_0}. \tag{29}$$

and

$$V \leqslant -\bar{\Omega}\big(V(t_0)+\bar{\Omega}\big)e^{t-t_0}. \tag{30}$$

As a result, by inequalities (26), (29) and (30), $V$is always bounded at any finite time interval $[t_0, t]$, that is, no finite-time escape occurs.

Step 3. According to Step 1, $\tilde{z}_x = \tilde{z}_v = 0, \forall t \geqslant T_1$. Then for $t \geqslant T_1$, the dynamics of the observation errors reduce to

$$\begin{cases} \dot{\eta}_x = \ \eta_v - \kappa_x\lceil H\eta_x\rfloor^{q_1} - \rho_x \mathrm{sign}(H\eta_x) \\ \dot{\eta}_v = \ -\kappa_v\lceil H\eta_v\rfloor^{q_1} - \rho_v \mathrm{sign}(H\eta_v) - \bar{u}_0, \end{cases} \tag{31}$$

First, we try the following Lyapunov function candidate

$$V_2 = \frac{1}{2}\eta_v^T H \eta_v. \tag{32}$$

Based on Lemma 4 and the fact that $\|\eta_v^T H\|_1 \geqslant \|\eta_v^T H\|_2$, we have

$$\begin{aligned} \dot{V}_2 &\leqslant -\eta_v^T H\bar{u}_0 - \kappa_v \eta_v^T H\lceil H\eta_v\rfloor^{q_1} - \rho_v \eta_v^T H \mathrm{sign}(H\eta_v) \\ &\leqslant -\kappa_v (mN)^{\frac{1-q_1}{2}} \|H\eta_v\|_2^{\frac{(q_1+1)}{2}} - (\rho_v - u_M)\|\eta_v^T H\|_1 \\ &\leqslant -\kappa_v (mN)^{\frac{1-q_1}{2}} \left(\frac{2\sigma^2_{\min}(H)}{\sigma_{\max}(H)}\right)^{\frac{(q_1+1)}{2}} V_2^{\frac{(q_1+1)}{2}} - (\rho_v - u_M)\left(\frac{2\sigma^2_{\min}(H)}{\sigma_{\max}(H)}\right)^{\frac{1}{2}} V_2^{\frac{1}{2}}. \end{aligned} \tag{33}$$

Therefore, the fixed-time convergence to the origin of η_v is verified by inequality (33) and Lemma 1 with the settling time bounded by T_2.

After the convergence of the observation error η_v, the dynamics of η_x can be reduced to

$$\dot{\eta}_x = -\kappa_x\lceil H\eta_x\rfloor^{q_1} - \rho_x \mathrm{sign}(H\eta_x). \tag{34}$$

Similarly, we obtain that the observation error η_x can converge to the origin within T_3.

Consequently, each follower can obtain the estimates of the leader's states x_0 and v_0 without the velocity measurements of the leader in fixed time T_0.

This completes the proof.

4.2. Radial basis function neural network approximator

Assume that the uncertain term $f_i(x_i, v_i) \in R^m$ can be expressed on a prescribed compact set $\Pi \in R^{2m}$ by

$$f_i(x_i, v_i) = \omega_i^T \phi_i(x_i, v_i) + \varepsilon_i, \tag{35}$$

where $\phi_i = \left[\phi_{i,1}^T, \phi_{i,2}^T, \ldots, \phi_{i,m}^T\right]^T$ with $\phi_{i,l}^T = \left[\phi_{i,l,1}^T, \phi_{i,l,2}^T, \ldots \phi_{i,l,\zeta_i}^T\right]^T \in R^{\zeta_i}, l = 1, 2, \ldots, m$ being a suitable set of ζ_i Gaussian functions. $\omega_i = \mathrm{diag}(\omega_{i,1}, \omega_{i,2}, \ldots, \omega_{i,m}) \in R^{m\zeta_i \times m}$ is the ideal RBFNN weight matrix with $\omega_{i,l} \in R^{\zeta_i}$, and ε_i is the RBFNN approximation error vector. To compensate for the unknown uncertainties, select the approximation of f_i as

$$\hat{f}_i(x_i, v_i) = \hat{\omega}_i^T \phi_i(x_i, v_i), \tag{36}$$

where $\hat{\omega}_i = \mathrm{diag}(\hat{\omega}_{i,1}, \hat{\omega}_{i,2}, \ldots, \hat{\omega}_{i,m}) \in R^{m\zeta_i \times m}$ with $\hat{\omega}_{i,l} \in R^{\zeta_i}$ is the current actual value vector of the RBFNN weight for the ith follower.

Besides, the error matrix of the RBFNN weights is defined as $\tilde{\omega}_i = \omega_i - \hat{\omega}_i$.

Remark 6. [50] According to Stone-Weierstrass approximation theorem, there exist positive numbers ω_M, ϕ_M and ε_M, such that $\|\omega_i\|_2 \leqslant \omega_M, \|\phi_i\|_2 \leqslant \phi_M$, and $\|\varepsilon_i\|_\infty \leqslant \varepsilon_M$.

4.3. Fixed-time adaptive control law design

In this subsection, the fixed-time adaptive control law will be designed by utilizing backstepping technique, after which the stability of the whole closed-loop multi-agent system will be presented.

Before designing the control law, define the auxiliary formation tracking position and velocity error e_{ix} and e_{iv} for the ith follower as

$$\begin{cases} e_{ix} = x_i - h_{ix} - \hat{x}_{0i} = x_i - h_{ix} - \tilde{x}_{0i} - x_{0i} \\ e_{iv} = v_i - h_{iv} - \hat{v}_{0i} = v_i - h_{iv} - \tilde{v}_{0i} - v_{0i}. \end{cases} \tag{37}$$

Substituting (20) into (37), the dynamics of e_{ix} and e_{iv} for the ith follower can be written as

$$\begin{cases} \dot{e}_{ix} = \ e_{iv} - \kappa_x\lceil \sum_{v_j\in N_i} a_{ij}(\tilde{x}_{0j} - \tilde{x}_{0i}) - b_i\tilde{x}_{0i}\rfloor^{q_1} \\ -\rho_x \mathrm{sign}\left(\sum_{v_j\in N_i} a_{ij}(\tilde{x}_{0j} - \tilde{x}_{0i}) - b_i\tilde{x}_{0i}\right) \\ \dot{e}_{iv} = \ -\kappa_v\lceil \sum_{v_j\in N_i} a_{ij}(\tilde{v}_{0j} - \tilde{v}_{0i}) - b_i\tilde{v}_{0i} + b_i\tilde{z}_v\rfloor^{q_1} \\ -\rho_v \mathrm{sign}\left(\sum_{v_j\in N_i} a_{ij}(\tilde{v}_{0j} - \tilde{v}_{0i}) - b_i\tilde{v}_{0i} + b_i\tilde{z}_v\right) \\ +f_i + u_i - \dot{h}_{iv}, i = 1, 2, \ldots, N. \end{cases} \tag{38}$$

First, taking e_{iv} as a virtual control input, then the virtual control law μ_i can be designed as

$$\mu_i = -\lambda_1\lceil e_{ix}\rfloor^{\varphi_1} - \lambda_2\lceil e_{ix}\rfloor^{\varphi_2}, \tag{39}$$

where $\lambda_1, \lambda_2 > 0, \varphi_1 > 1, 0 < \varphi_2 < 1$.

Choose a Lyapunov function as follows

$$V_3 = \frac{1}{2}e_{ix}^T e_{ix}. \tag{40}$$

The time differentiation of (40) yields that

$$\begin{aligned} \dot{V}_3 = \ & e_{ix}^T \dot{e}_{ix} \\ = \ & e_{ix}^T \Bigg(-\lambda_1\lceil e_{ix}\rfloor^{\varphi_1} - \lambda_2\lceil e_{ix}\rfloor^{\varphi_2} - \kappa_x\lceil \sum_{v_j\in N_i} a_{ij}(\tilde{x}_{0j} - \tilde{x}_{0i}) - b_i\tilde{x}_{0i}\rfloor^{q_1} \\ & - \rho_x \mathrm{sign}\left(\sum_{v_j\in N_i} a_{ij}(\tilde{x}_{0j} - \tilde{x}_{0i}) - b_i\tilde{x}_{0i}\right)\Bigg). \end{aligned} \tag{41}$$

From Theorem 1, both the observation error $\tilde{x}_{0j}$ and $\tilde{x}_{0i}$ are always bounded. Thus, by utilizing Young's inequality, the following inequality holds for a positive constant Δ_1.

$$\begin{aligned} & e_{ix}^T\left(-\kappa_x\lceil \sum_{v_j\in N_i} a_{ij}(\tilde{x}_{0j} - \tilde{x}_{0i}) - b_i\tilde{x}_{0i}\rfloor^{q_1} - \rho_x \mathrm{sign}\left(\sum_{v_j\in N_i} a_{ij}(\tilde{x}_{0j} - \tilde{x}_{0i}) - b_i\tilde{x}_{0i}\right)\right) \\ & \leqslant \tfrac{1}{2}e_{ix}^T e_{ix} + \Delta_1. \end{aligned} \tag{42}$$

Invoking Lemmas 3 and 4, $\dot{V}_3$ develops to

$$\begin{aligned} \dot{V}_3 \leqslant \ & -2^{\frac{\varphi_1+1}{2}} m^{\frac{1-\varphi_1}{2}} \lambda_1 V_3^{\frac{\varphi_1+1}{2}} - 2^{\frac{\varphi_2+1}{2}} \lambda_2 V_3^{\frac{\varphi_2+1}{2}} \\ & + V_3 + \Delta_1 \\ \leqslant \ & -\left(2^{\frac{\varphi_1+1}{2}} m^{\frac{1-\varphi_1}{2}} \lambda_1 - 1\right) V_3^{\frac{\varphi_1+1}{2}} + \Delta_1 \\ & -\left(2^{\frac{\varphi_2+1}{2}} \lambda_2 - 1\right) V_3^{\frac{\varphi_2+1}{2}}. \end{aligned} \tag{43}$$

The last inequality is obtained based on the fact that $V_3 \leqslant V_3^{\frac{\varphi_1+1}{2}} + V_3^{\frac{\varphi_2+1}{2}}$. According to the above inequality and Le-mma 2, e_{ix} will converge to a small neighborhood of the origin within fixed time. Thus, e_{ix} will always be bounded at any finite time interval $[t_0, t]$. Recalling Theorem 1, the observation error $\tilde{x}_{0j} = \tilde{x}_{0i} = 0$ for all $t \geqslant T_0$. Thus, for $t \geqslant T_0$, inequality (43) reduces to

$$\dot{V}_3 \leqslant -2^{\frac{\varphi_1+1}{2}} m^{\frac{1-\varphi_1}{2}} \lambda_1 V_3^{\frac{\varphi_1+1}{2}} - 2^{\frac{\varphi_2+1}{2}} \lambda_2 V_3^{\frac{\varphi_2+1}{2}}. \tag{44}$$

According to Lemma 1, e_{ix} will converge to the origin in fixed time.

Next, we introduce a new state μ_{id} , which is obtained by the following nonlinear nonsmooth filter:

$$\tau_i \dot{\mu}_{id} = \lceil \mu_i - \mu_{id} \rfloor^{\varphi_1} + \lceil \mu_i - \mu_{id} \rfloor^{\varphi_2}, \mu_{id}(t_0) = \mu_i(t_0), \tag{45}$$

where the filter parameter τ_i is a small positive constant.

Then, to backstep, define the tracking error as $\xi_i = e_{iv} - \mu_{id}$. The dynamics of e_{ix} and ξ_i are written as

$$\begin{cases} \dot{e}_{ix} = \xi_i + \mu_{id} - \kappa_x \lceil \sum_{v_j \in N_i} a_{ij}(\tilde{x}_{0j} - \tilde{x}_{0i}) - b_i \tilde{x}_{0i} \rfloor^{q_1} \\ -\rho_x \mathrm{sign}\left(\sum_{v_j \in N_i} a_{ij}(\tilde{x}_{0j} - \tilde{x}_{0i}) - b_i \tilde{x}_{0i} \right) \\ \dot{\xi}_i = -\kappa_v \lceil \sum_{v_j \in N_i} a_{ij}(\tilde{v}_{0j} - \tilde{v}_{0i}) - b_i \tilde{v}_{0i} + b_i \tilde{z}_v \rfloor^{q_1} \\ -\rho_v \mathrm{sign}\left(\sum_{v_j \in N_i} a_{ij}(\tilde{v}_{0j} - \tilde{v}_{0i}) - b_i \tilde{v}_{0i} + b_i \tilde{z}_v \right) + f_i + u_i - \dot{h}_{iv} - \dot{\mu}_{id}. \end{cases} \tag{46}$$

Therefore, the actual control law for the ith follower is designed as

$$u_i = -\gamma_1 \lceil \xi_i \rfloor^{\varphi_1} - \gamma_2 \lceil \xi_i \rfloor^{\varphi_2} - \hat{\omega}_i^T \phi_i + \dot{h}_{iv} + \dot{\mu}_{id}, i = 1, 2, \ldots, N, \tag{47}$$

where $\gamma_1, \gamma_2 > 0$, and $\dot{\mu}_{id}$ is obtained by (45).

The corresponding adaptive law is designed as

$$\dot{\hat{w}}_i = F_i \tilde{\phi}_i \tilde{\xi}_i^T - F_i \vartheta_i \hat{w}_i, i = 1, 2, \ldots, N, \tag{48}$$

where $F_i, \vartheta_i > 0, \tilde{\phi}_i = \mathrm{diag}(\phi_{i,1}, \phi_{i,2}, \ldots, \phi_{i,m}), \tilde{\xi}_i = \mathrm{diag}(\xi_{i,1}, \xi_{i,2}, \ldots, \xi_{i,m})$ with $\xi_{i,a}$ being the ath element of the vector $\xi_i, a = 1, 2, \ldots, m$.

Define the filtering error of the nonsmooth filter (45) as

$$e_{\mu_i} = \mu_i - \mu_{id}, \tag{49}$$

The time differentiation of (49) yields that

$$\dot{e}_{\mu_i} = -(\lceil e_{\mu_i} \rfloor^{\varphi_1} + \lceil e_{\mu_i} \rfloor^{\varphi_2})/\tau_i + \dot{\mu}_i. \tag{50}$$

Construct the following Lyapunov function

$$V_4 = V_3 + \frac{1}{2}\xi_i^T \xi_i + \frac{1}{2}\mathrm{tr}\left(\tilde{\omega}_i^T F_i^{-1} \tilde{\omega}_i\right) + \frac{1}{2} e_{\mu_i}^T e_{\mu_i}. \tag{51}$$

Invoking $y_1^T y_2 = \mathrm{tr}(y_2 y_1^T), \forall y_1, y_2 \in R^n$, the derivative of V_4 with respect to time is

$$\begin{aligned} \dot{V}_4 &= e_{ix}^T \dot{e}_{ix} + \xi_i^T \dot{\xi}_i + \tilde{\omega}_i^T F_i^{-1} \dot{\tilde{\omega}}_i + e_{\mu_i}^T \dot{e}_{\mu_i} \\ &= e_{ix}^T \Bigg(-\lambda_1 \lceil e_{ix} \rfloor^{\varphi_1} - \lambda_2 \lceil e_{ix} \rfloor^{\varphi_2} - e_{\mu_i} + \xi_i - \kappa_x \lceil \sum_{v_j \in N_i} a_{ij}(\tilde{x}_{0j} - \tilde{x}_{0i}) - b_i \tilde{x}_{0i} \rfloor^{q_1} \\ &\quad - \rho_x \mathrm{sign}\left(\sum_{v_j \in N_i} a_{ij}(\tilde{x}_{0j} - \tilde{x}_{0i}) - b_i \tilde{x}_{0i} \right) \Bigg) \\ &\quad + \xi_i^T \Bigg(-\gamma_1 \lceil \xi_i \rfloor^{\varphi_1} - \gamma_2 \lceil \xi_i \rfloor^{\varphi_2} - \kappa_v \lceil \sum_{v_j \in N_i} a_{ij}(\tilde{v}_{0j} - \tilde{v}_{0i}) - b_i \tilde{v}_{0i} + b_i \tilde{z}_v \rfloor^{q_1} \\ &\quad - \rho_v \mathrm{sign}\left(\sum_{v_j \in N_i} a_{ij}(\tilde{v}_{0j} - \tilde{v}_{0i}) - b_i \tilde{v}_{0i} + b_i \tilde{z}_v \right) \Bigg) + \mathrm{tr}(\tilde{\omega}_i^T \phi_i \xi_i^T) \\ &\quad + \mathrm{tr}\left(\tilde{\omega}_i^T F_i^{-1} \dot{\tilde{\omega}}_i\right) + \xi_i^T \varepsilon_i + e_{\mu_i}^T (-(\lceil e_{\mu_i} \rfloor^{\varphi_1} + \lceil e_{\mu_i} \rfloor^{\varphi_2})/\tau_i + \dot{\mu}_i). \end{aligned} \tag{52}$$

Recalling (42), (47) and (48), we can get

$$\begin{aligned} \dot{V}_4 \leqslant\ & -\lambda_1 e_{ix}^T \lceil e_{ix} \rfloor^{\varphi_1} - \lambda_2 e_{ix}^T \lceil e_{ix} \rfloor^{\varphi_2} + e_{ix}^T \xi_i + \tfrac{1}{2} e_{ix}^T e_{ix} \\ & -\kappa_v \xi_i^T \lceil \sum_{v_j \in N_i} a_{ij}(\tilde{v}_{0j} - \tilde{v}_{0i}) - b_i \tilde{v}_{0i} + b_i \tilde{z}_v \rfloor^{q_1} \\ & -\rho_v \xi_i^T \mathrm{sign}\left(\sum_{v_j \in N_i} a_{ij}(\tilde{v}_{0j} - \tilde{v}_{0i}) - b_i \tilde{v}_{0i} + b_i \tilde{z}_v \right) \\ & -\gamma_1 \xi_i^T \lceil \xi_i \rfloor^{\varphi_1} - \gamma_2 \xi_i^T \lceil \xi_i \rfloor^{\varphi_2} + \vartheta_i \mathrm{tr}(\tilde{\omega}_i^T \hat{\omega}_i) \\ & + e_{\mu_i}^T (-(\lceil e_{\mu_i} \rfloor^{\varphi_1} + \lceil e_{\mu_i} \rfloor^{\varphi_2})/\tau_i + \dot{\mu}_i) \\ & + \Delta_1 + \xi_i^T \varepsilon_i + e_{ix}^T e_{\mu_i}. \end{aligned} \tag{53}$$

Theorem 2. *Considering the multi-agent system with Nfollowers (9) and one leader (10). Suppose Assumptions 1–3 hold. Then under the control law (47) and the adaptive law (48), the multi-agent system can achieve the expected time-varying formation in fixed time* $T_4 \leqslant \frac{1}{(\varphi_1 - 1)c_1\phi} + \frac{2}{c_2\phi(1-\varphi_2)} + T_0$ *with* $c_1 = \min\left\{2^{\frac{\varphi_1+1}{2}} m^{\frac{1-\varphi_1}{2}} \lambda_1 - 2, 2^{\frac{\varphi_1+1}{2}} m^{\frac{1-\varphi_1}{2}} \gamma_1 - \frac{5}{4}, 1, \frac{1}{\tau_i} 2^{\frac{\varphi_1+1}{2}} m^{\frac{1-\varphi_1}{2}} - 1\right\}$ *and* $c_2 = \min\left\{2^{\frac{\varphi_2+1}{2}} \gamma_2 - 2, 2^{\frac{\varphi_2+1}{2}} \gamma_2 - \frac{5}{4}, \frac{1}{\tau_i} 2^{\frac{\varphi_2+1}{2}} - 1, 1\right\}$ *, if the following condition is satisfied:*

$$\begin{cases} 2^{\frac{\varphi_1+1}{2}} m^{\frac{\varphi_1-1}{2}} \lambda_1 - 3 > 0 \\ 2^{\frac{\varphi_2+1}{2}} \lambda_2 - 3 > 0 \\ 2^{\frac{\varphi_1+1}{2}} m^{\frac{\varphi_1-1}{2}} \gamma_1 - \frac{9}{4} > 0 \\ 2^{\frac{\varphi_2+1}{2}} \gamma_2 - \frac{9}{4} > 0 \\ \frac{1}{\tau_i} 2^{\frac{\varphi_1+1}{2}} m^{\frac{1-\varphi_1}{2}} - 1 > 0 \\ \frac{1}{\tau_i} 2^{\frac{\varphi_2+1}{2}} - 1 > 0 \end{cases} \tag{54}$$

Proof. The proof contains two steps. First, we prove $e_{ix}, \xi_i, \tilde{\omega}_i$ and e_{μ_i} are UUB. Then, we prove that $e_{ix}, e_{iv}, \tilde{\omega}_i$ and e_{μ_i} can converge to a small region around the origin in fixed time T_4 .

Step 1. Recalling Theorem 1, the observation errors $\tilde{x}_{0i}, \tilde{v}_{0i}$ and $\tilde{z}_v$ are always bounded. Therefore, the following inequality holds for a positive constant Δ_2

$$\begin{aligned} & -\kappa_v \xi_i^T \lceil \sum_{v_j \in N_i} a_{ij}(\tilde{v}_{0j} - \tilde{v}_{0i}) - b_i \tilde{v}_{0i} + b_i \tilde{z}_v \rfloor^{q_1} \\ & -\rho_v \xi_i^T \mathrm{sign}\left(\sum_{v_j \in N_i} a_{ij}(\tilde{v}_{0j} - \tilde{v}_{0i}) - b_i \tilde{v}_{0i} + b_i \tilde{z}_v \right) \\ & \leqslant \tfrac{1}{2} \xi_i^T \xi_i + \Delta_2. \end{aligned} \tag{55}$$

Based on the above inequality and using Young's inequality, (53) can be rewritten as

$$\begin{aligned} \dot{V}_4 \leqslant\ & -\lambda_1 e_{ix}^T \lceil e_{ix} \rfloor^{\varphi_1} - \lambda_2 e_{ix}^T \lceil e_{ix} \rfloor^{\varphi_2} + e_{ix}^T \xi_i + \tfrac{1}{2} e_{ix}^T e_{ix} \\ & -\gamma_1 \xi_i^T \lceil \xi_i \rfloor^{\varphi_1} - \gamma_2 \xi_i^T \lceil \xi_i \rfloor^{\varphi_2} + \mathrm{tr}(\tilde{\omega}_i^T \hat{\omega}_i) + \Delta_1 \\ & + \tfrac{1}{2} \xi_i^T \xi_i + \Delta_2 + \tfrac{1}{8} \xi_i^T \xi_i + 2\varepsilon_M^2 + e_{ix}^T e_{\mu_i} \\ & + e_{\mu_i}^T (-(\lceil e_{\mu_i} \rfloor^{\varphi_1} + \lceil e_{\mu_i} \rfloor^{\varphi_2})/\tau_i + \dot{\mu}_i) \end{aligned} \tag{56}$$

Similar to [51–53], we assume that there exists a positive constant μ_{iM} such that $\|\dot{\mu}_i\|_2 \leqslant \mu_{iM}$. Then we can get

$$e_{\mu_i}^T \dot{\mu}_i \leqslant \frac{1}{2} e_{\mu_i}^T e_{\mu_i} + \frac{1}{2} \mu_{iM}^2 \tag{57}$$

Furthermore, we obtain that

$$\begin{aligned}\dot V_4 \leqslant\ & -\lambda_1 e_{ix}^T\lceil e_{ix}\rfloor^{\varphi_1} - \lambda_2 e_{ix}^T\lceil e_{ix}\rfloor^{\varphi_2} + \tfrac{3}{2}e_{ix}^T e_{ix}\\ & -\gamma_1\xi_i^T\lceil\xi_i\rfloor^{\varphi_1} - \gamma_2\xi_i^T\lceil\xi_i\rfloor^{\varphi_2} + \tfrac{9}{8}\xi_i^T\xi_i + \tfrac{1}{2}\mu_{iM}^2\\ & +\Delta_1+\Delta_2+2\varepsilon_M^2 - \mathrm{tr}(\tilde\omega_i^T\tilde\omega_i) + \mathrm{tr}(\tilde\omega_i^T\omega_i)\\ & -\tfrac{1}{\tau_i}e_{\mu_i}^T\lceil e_{\mu_i}\rfloor^{\varphi_1+1} - \tfrac{1}{\tau_i}e_{\mu_i}^T\lceil e_{\mu_i}\rfloor^{\varphi_2+1} + \tfrac{1}{2}e_{\mu_i}^T e_{\mu_i}.\end{aligned} \tag{58}$$

By utilizing Lemmas 3,4, we get

$$\begin{aligned}\dot V_4 \leqslant\ & -\left(2^{\frac{\varphi_1+1}{2}}m^{\frac{1-\varphi_1}{2}}\lambda_1 - 3\right)\left(\tfrac{1}{2}e_{ix}^Te_{ix}\right)^{\frac{\varphi_1+1}{2}}\\ & -\left(2^{\frac{\varphi_2+1}{2}}\lambda_2 - 3\right)\left(\tfrac{1}{2}e_{ix}^Te_{ix}\right)^{\frac{\varphi_2+1}{2}}\\ & -\left(2^{\frac{\varphi_1+1}{2}}m^{\frac{1-\varphi_1}{2}}\gamma_1 - \tfrac{9}{4}\right)\left(\tfrac{1}{2}\xi_i^T\xi_i\right)^{\frac{\varphi_1+1}{2}}\\ & -\left(2^{\frac{\varphi_2+1}{2}}\gamma_2 - \tfrac{9}{4}\right)\left(\tfrac{1}{2}\xi_i^T\xi_i\right)^{\frac{\varphi_2+1}{2}}\\ & -\left(\tfrac{1}{\tau_i}2^{\frac{\varphi_1+1}{2}}m^{\frac{1-\varphi_1}{2}} - 1\right)\left(\tfrac{1}{2}e_{\mu_i}^Te_{\mu_i}\right)^{\frac{\varphi_1+1}{2}}\\ & -\left(\tfrac{1}{\tau_i}2^{\frac{\varphi_2+1}{2}} - 1\right)\left(\tfrac{1}{2}e_{\mu_i}^Te_{\mu_i}\right)^{\frac{\varphi_2+1}{2}}\\ & -\tfrac{1}{2}\mathrm{tr}(\tilde\omega_i^T\tilde\omega_i) + \Delta\\ \leqslant\ & -\tfrac{1}{2}\lambda_{\min}e_{ix}^Te_{ix} - \tfrac{1}{2}\gamma_{\min}\xi_i^T\xi_i - \tfrac{1}{2}\mathrm{tr}(\tilde\omega_i^T\tilde\omega_i)\\ & -\tfrac{1}{2}\tau_{\min}e_{\mu_i}^Te_{\mu_i} + \Delta\\ \leqslant\ & -\varrho V_4 + \Delta,\end{aligned} \tag{59}$$

where $\Delta = \Delta_1+\Delta_2+\frac{1}{2}\omega_M^2+\frac{1}{2}\mu_{iM}^2+2\varepsilon_M^2$, $\lambda_{\min} = \min\left\{2^{\frac{\varphi_1+1}{2}}m^{\frac{1-\varphi_1}{2}}\lambda_1 - 3, 2^{\frac{\varphi_2+1}{2}}\lambda_2 - 3\right\}$, $\gamma_{\min} = \min\left\{2^{\frac{\varphi_1+1}{2}}m^{\frac{1-\varphi_1}{2}}\gamma_1 - \frac{9}{4}, 2^{\frac{\varphi_2+1}{2}}\gamma_2 - \frac{9}{4}\right\}$, $\tau_{\min} = \min\left\{\frac{1}{\tau_i}2^{\frac{\varphi_1+1}{2}}m^{\frac{1-\varphi_1}{2}} - 1, \frac{1}{\tau_i}2^{\frac{\varphi_2+1}{2}} - 1\right\}$, $\varrho = \min\{\lambda_{\min},\gamma_{\min},\tau_{\min},\frac{1}{2}\}$.

It yields that

$$V_4 \leqslant \frac{\Delta}{\varrho} + \left(V_4(t_0) - \frac{\Delta}{\varrho}\right)e^{-\varrho(t-t_0)}. \tag{60}$$

The above inequality indicates that variates e_{ix}, ξ_i, e_{μ_i} and $\tilde\omega_i$ are UUB, which means $e_{ix}, e_{iv}, e_{\mu_i}$ and $\tilde\omega_i$ are UUB.

Step 2. From Step 1, we can obtain that there exists a positive constant $\tilde\omega_M$ such that $\|\tilde\omega\|_2 \leqslant \tilde\omega_M$. In addition, from Theorem 1, $\tilde x_{0i} = \tilde v_{0i} = \tilde z_v = 0$ for all $t \geqslant T_0$. Hence, for $t \geqslant T_0$, the following inequality can be derived:

$$\begin{aligned}\dot V_4 \leqslant\ & -\left(2^{\frac{\varphi_1+1}{2}}m^{\frac{1-\varphi_1}{2}}\lambda_1 - 2\right)\left(\tfrac{1}{2}e_{ix}^Te_{ix}\right)^{\frac{\varphi_1+1}{2}}\\ & -\left(2^{\frac{\varphi_2+1}{2}}\lambda_2 - 2\right)\left(\tfrac{1}{2}e_{ix}^Te_{ix}\right)^{\frac{\varphi_2+1}{2}}\\ & -\left(2^{\frac{\varphi_1+1}{2}}m^{\frac{1-\varphi_1}{2}}\gamma_1 - \tfrac{5}{4}\right)\left(\tfrac{1}{2}\xi_i^T\xi_i\right)^{\frac{\varphi_1+1}{2}}\\ & -\left(2^{\frac{\varphi_2+1}{2}}\gamma_2 - \tfrac{5}{4}\right)\left(\tfrac{1}{2}\xi_i^T\xi_i\right)^{\frac{\varphi_2+1}{2}}\\ & -\left(\tfrac{1}{\tau_i}2^{\frac{\varphi_1+1}{2}}m^{\frac{1-\varphi_1}{2}} - 1\right)\left(\tfrac{1}{2}e_{\mu_i}^Te_{\mu_i}\right)^{\frac{\varphi_1+1}{2}}\\ & -\left(\tfrac{1}{\tau_i}2^{\frac{\varphi_2+1}{2}} - 1\right)\left(\tfrac{1}{2}e_{\mu_i}^Te_{\mu_i}\right)^{\frac{\varphi_2+1}{2}}\\ & -\left(\tfrac{1}{2}\mathrm{tr}\left(\tilde\omega_i^TF_i^{-1}\tilde\omega_i\right)\right)^{\frac{\varphi_1+1}{2}} - \left(\tfrac{1}{2}\mathrm{tr}\left(\tilde\omega_i^TF_i^{-1}\tilde\omega_i\right)\right)^{\frac{\varphi_2+1}{2}}\\ & +\left(\tfrac{1}{2}\mathrm{tr}\left(\tilde\omega_i^TF_i^{-1}\tilde\omega_i\right)\right)^{\frac{\varphi_1+1}{2}} + \left(\tfrac{1}{2}\mathrm{tr}\left(\tilde\omega_i^TF_i^{-1}\tilde\omega_i\right)\right)^{\frac{\varphi_2+1}{2}}\\ & -\tfrac{1}{2}\mathrm{tr}(\tilde\omega_i^T\tilde\omega_i) + \Delta.\end{aligned} \tag{61}$$

Let $\bar\Delta = \left(\frac{1}{2}\mathrm{tr}\left(\tilde\omega_i^TF_i^{-1}\quad\tilde\omega_i\right)\right)^{\frac{\varphi_1+1}{2}} + \left(\frac{1}{2}\mathrm{tr}\left(\tilde\omega_i^TF_i^{-1}\tilde\omega_i\right)\right)^{\frac{\varphi_2+1}{2}} - \frac{1}{2}\mathrm{tr}(\tilde\omega_i^T\tilde\omega_i) + \frac{1}{2}\omega_M^2 + \frac{1}{2}\mu_{iM}^2 + 2\varepsilon_M^2$. Since $\|\tilde\omega\|$ is UUB, there exists a positive constant $\bar\Delta_M$ such that $\bar\Delta \leqslant \bar\Delta_M$, Then (61) can be rewritten as:

$$\begin{aligned}\dot V_4 \leqslant\ & -c_1\left(\tfrac{1}{2}e_{ix}^Te_{ix}\right)^{\frac{\varphi_1+1}{2}} + \left(\tfrac{1}{2}\xi_i^T\xi_i\right)^{\frac{\varphi_1+1}{2}}\\ & -c_1\left(\left(\tfrac{1}{2}e_{\mu_i}^Te_{\mu_i}\right)^{\frac{\varphi_1+1}{2}} + \left(\tfrac{1}{2}\mathrm{tr}\left(\tilde\omega_i^TF_i^{-1}\tilde\omega_i\right)\right)^{\frac{\varphi_1+1}{2}}\right)\\ & -c_2\left(\left(\tfrac{1}{2}e_{ix}^Te_{ix}\right)^{\frac{\varphi_2+1}{2}} + \left(\tfrac{1}{2}\xi_i^T\xi_i\right)^{\frac{\varphi_2+1}{2}}\right)\\ & -c_2\left(\left(\tfrac{1}{2}e_{\mu_i}^Te_{\mu_i}\right)^{\frac{\varphi_2+1}{2}} + \left(\tfrac{1}{2}\mathrm{tr}\left(\tilde\omega_i^TF_i^{-1}\tilde\omega_i\right)\right)^{\frac{\varphi_2+1}{2}}\right)\\ & +\bar\Delta_M.\\ \leqslant\ & -2^{1-\varphi_1}c_1(V_4)^{\frac{\varphi_1+1}{2}} - c_2(V_4)^{\frac{\varphi_2+1}{2}} + \bar\Delta_M.\end{aligned} \tag{62}$$

According to Lemma 2, we can obtain that $X_i = \left[\|e_{ix}\|_2, \|\xi_i\|_2, \|\tilde\omega_i\|_2, \|e_{\mu_i}^T\|_2\right]^T$ is practical fixed-time stable and will converge to the following compact set Ω_1 within fixed time T_4 .

$$\Omega_1 = \left\{X_i | V_4(X_i) \leqslant \min\left\{\left(\frac{\bar\Delta_M}{(1-\phi)c_1}2^{\varphi_1-1}\right)^{\frac{2}{\varphi_1+1}}, \left(\frac{\bar\Delta_M}{(1-\phi)c_2}\right)^{\frac{2}{\varphi_2+1}}\right\}\right\}. \tag{63}$$

Since $e_{ix} = \delta_{ix}$ and $e_{iv} = \delta_{iv}$ for $t \geqslant T_0$, we can conclude that δ will converge to a small compact set by appropriately selecting the control parameters within fixed time T_4 . Therefore, the multi-agent system can achieve the expected time-varying formation within fixed time T_4 .

This completes the proof.

Remark 7. From Theorem 2, the formation tracking errors can converge to a small region around the origin in fixed time in presence of uncertainties under the proposed control scheme. As a matter of fact, most adaptive NN formation/ consensus control for multi-agent systems achieve that the tracking errors are UUB or convergent in finite time [31,46,50,54]. Consequently, the proposed novel formation control scheme can improve the formation control performance compared to the aforementioned results.

Remark 8. By proposing the nonlinear nonsmooth filter (45), the singular problem brought from the item $\lceil\mu_i - \mu_{id}\rfloor^{\varphi_2}$ is well solved, as well as the "explosion of complexity" problem. In addition, compared to the first-order traditional filters, filter (45) can ensure the fixed-time convergence of the filtering error.

Remark 9. By Theorem 2, it follows that $\|X_i\|_2 \leqslant x_M + \|h_i\|_2 + \Delta_3$ with $X_i = [x_i^T, v_i^T]^T$ holds for positive number Δ_3 at any finite time interval $[t_0, t]$. According to Assumption 3, at any finite time interval $[t_0, t]$, the compact approximation region Π of the ith RBFNN can be chosen as $\Pi = \{X_i | \|X_i\| \leqslant x_M + \|h_i\|_2 + \Delta_3\}, i = 1, 2, \ldots, N$.

Remark 10. As a matter of fact, the observer and control parameters are selected according to the theoretical results and engineering characteristics. For the observer parameters, the positive constants $\beta, \alpha_1, \alpha_2$ need to satisfy condition (13), and $q_1, q_2 > 1$. Other observer gains $\kappa_x, \kappa_v, \rho_x, \rho_v$ should be positive and $\rho_v > u_M$. Besides, larger values of $\kappa_x, \kappa_v, \rho_x, \rho_v$ increase the convergence rates at a cost of larger chattering. Therefore, we need to tune the gains $\kappa_x, \kappa_v, \rho_x, \rho_v$ to make a balance between rapidity and smoothness. For the control parameters, $\lambda_1, \lambda_2, \varphi_1, \varphi_2, \gamma_1, \gamma_2, \tau_i$ are positive and required to satisfy condition (54). Furthermore, we should tune the control gains $\lambda_1, \lambda_2, \gamma_1, \gamma_2$ to make a tradeoff among the formation tracking error, rapidity, and smoothness. The filter parameter τ_i should be chosen to be small enough and keep a balance between the filtering error and the smoothness. F_i and ϑ_i in the adaptive law are positive constants. In addition, the parameters F_i and ϑ_i also need to be tuned to keep a balance between the learning rates, the approximation error and smoothness.

Remark 11. Actually, the proposed fixed-time formation control scheme operates well under the condition that the communication network is benign and known beforehand, just similar to many existing works about fixed-time control for multi-agent systems. However, the communication network cannot always be benign, and may suffer from cyberattacks [55]. Therefore, the fixed-time formation control for multi-agent systems under deception attacks is worthy to be deeply investigated. Following the idea in [55], we will do our best to design a novel fixed-time formation control scheme for multi-agent systems under deception attacks in the future.

5. Simulation results

Construct a multi-agent system with six followers whose dynamics are described by (9) and one leader whose dynamics are described by (10). Choose the graph G_0 depicting the information flow among the followers and the leader, as shown in Fig.1.

The six followers are supposed to keep a periodic time-varying regular hexagon formation in the X-Y plane and at the same time to keep rotating around the time-varying leader with

$$x_0(t) = \begin{cases} \left[5t + \frac{15}{2}, 10\cos(0.2t)\right]^T, & 3s \leqslant t \leqslant 30s, \\ \left[\frac{5}{6}t^2, 10\cos(0.2t)\right]^T, & 0s \leqslant t < 3s. \end{cases} \tag{64}$$

Thus, in the case of $m = 2$, x_i and v_i can be rewritten as $x_i = [x_{iX}, x_{iY}]^T$ and $v_i = [v_{iX}, v_{iY}]^T$, respectively. Other state vectors can be rewritten in the same way. Moreover, the uncertainties f_i are selected as

$$\begin{aligned} f_1 &= [4\sin(0.2v_{iX}), 4\cos(0.1v_{iY})]^T, \\ f_2 &= [4\cos(0.2v_{iX}), 4\cos(0.2v_{iY})]^T, \\ f_3 &= [4\sin(0.1v_{iX}^2), 4\cos(0.1v_{iY}^2)]^T, \\ f_4 &= [4\sin(0.1v_{iX}^2), 4\cos(0.1v_{iY}^2)]^T, \\ f_5 &= [4\sin(0.1v_{iX}^2), 4\cos(0.1v_{iY}^2)]^T, \\ f_6 &= [4\sin(0.2v_{iX}^2), 4\cos(0.1v_{iY}^2)]^T. \end{aligned} \tag{65}$$

In addition, the time-varying formation is specified by

$$h_{ix}(t) = \begin{bmatrix} 0.2t\cos(0.1t + (i-1)\pi/3) \\ 0.2t\sin(0.1t + (i-1)\pi/3) \end{bmatrix}, \tag{66}$$

The selected values of the observer and control parameters are shown in Table 1 and Table 2, respectively. The initial position states of the six followers and the leader are set as $x_1(0) = [4,6]^T, x_2(0) = [2,1]^T, x_3(0) = [3,6]^T, x_4(0) = [5,3]^T, x_5(0) = [4,4]^T$, $x_6(0) = [5,2]^T, x_0(0) = [0,10]^T$. The initial velocity states of the six followers and the leader are set as zero vectors. Moreover, the number of nodes in each NN is chosen as $\zeta_i = 5$. The initial values of the states of the FTCLSO consisting of (11) and (12) are all set as zero, except that the initial values of $\hat{v}_{02}$ and $\hat{v}_{04}$ are chosen as $\hat{v}_{02}(t_0) = 5$ and $\hat{v}_{04}(t_0) = 3$, respectively. The simulation results are presented by 2–6. Fig. 2 shows the varying positions of the six followers and the leader at $t = 10, 15, 20, 25, 30s$. It is observed from the results that the six followers successfully keep a time-varying regular hexagon formation with varying edges while keeping rotating around the dynamic leader and tracking the trajectory of the leader. Fig. 3 represents the formation tracking position errors δ_{ix} of each follower on X-axis and Y-axis, while Fig. 4 presents the observation errors of the position and the velocity on X-axis and Y-axis, respectively. From Figs. 3,4, it can be obtained that the formation tracking errors converge to a small neighbourhood of zero within 5s, while the observation errors of position and velocity converge to zero at around 3s. The fast convergence rates show the superiority of fixed-time control scheme. In addition, the chattering happens in Fig. 4 resulting from the discontinuous terms in(11) and (12). Fig. 5 displays the NN approximation errors of each follower on X-axis and Y-axis. From Fig. 5, it can be seen that the unknown

Table 1
Observer parameters.

Parameters	Values	Parameters	Values
α_1	4	ρ_x	1
α_2	4	ρ_v	2
β	2	q_1	2
κ_x	3	q_2	2
κ_v	1		

Table 2
Control parameters.

Parameters	Values	Parameters	Values
γ_1	0.6	τ_i	0.25
γ_2	2	λ_1	1
φ_1	2	λ_2	3
φ_2	0.8	ϑ_1	0.001
F_1	2	ϑ_2	0.01
F_2	3	ϑ_3	0.001
F_3	3	ϑ_4	0.001
F_4	5	ϑ_5	0.01
F_5	5	ϑ_6	0.001
F_6	5		

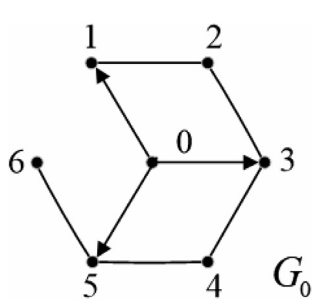

Fig. 1. The interaction graph.

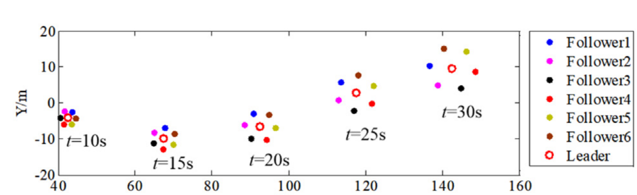

Fig. 2. Position snapshots of the six followers and the leader.

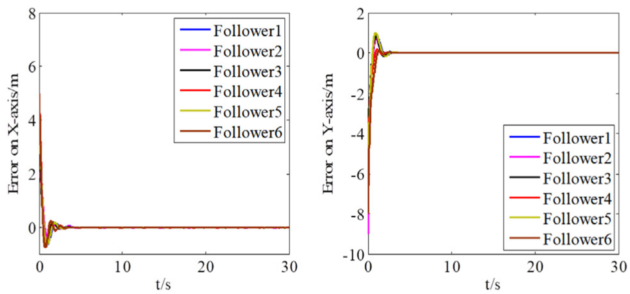

Fig. 3. Formation tracking position errors on X-axis and Y-axis of the six followers.

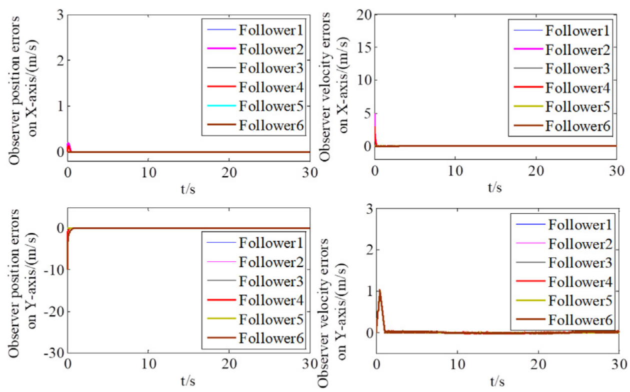

Fig. 4. Observation errors of the six followers on X-axis and Y-axis.

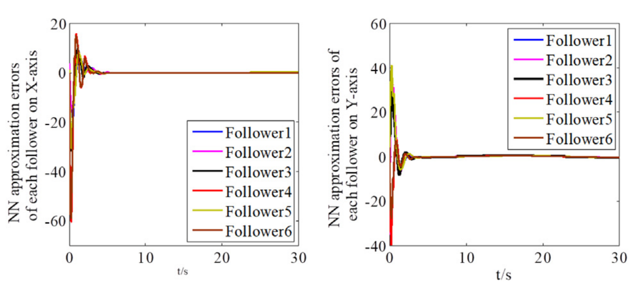

Fig. 5. NN approximation errors on X-axis and Y-axis of the six followers.

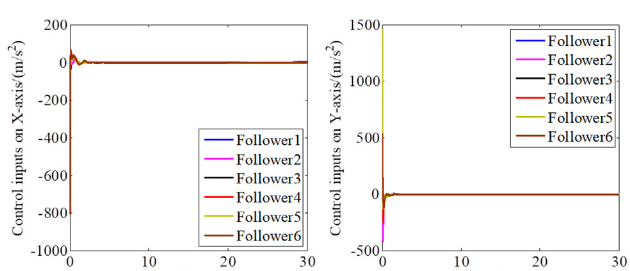

Fig. 6. Control inputs on X-axis and Y-axis of the six followers.

uncertainties are well approximated by RBFNNs. Fig. 6 shows the curves of the control inputs of the six followers on X-axis and Y-axis, from which we can see that the singularity problem does not happen.

To show the superiority of the fixed-time control, one more simulation is conducted under different initial states of the six followers. In this case, the initial position states of the six followers are set as $x_1(0) = [-2, 10]^T, x_2(0) = [2, 10]^T, x_3(0) = [-2, 0]^T, x_4(0) = [0, 5]^T, x_5(0) = [-2, 0]^T, x_6(0) = [-2, -5]^T$. Fig. 7 represents the formation tracking position errors on X-axis and Y-axis of the six followers under different initial states. By comparing Fig. 3 and Fig. 7, it can be observed that the formation tracking position errors converge to a small enough region around zero within a similar settling time although the transient processes are quite different. Therefore, it can be concluded that the formation position errors can converge to a small enough region around zero within fixed time independent of their initial states under the proposed fixed-time formation control scheme.

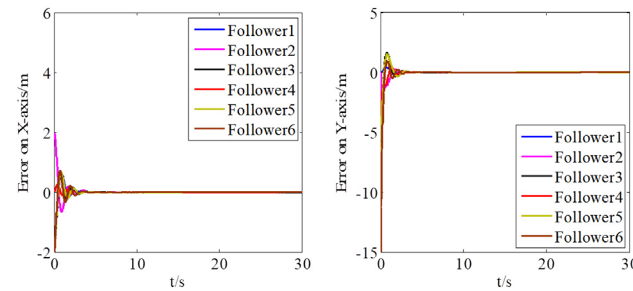

Fig. 7. Formation tracking position errors on X-axis and Y-axis of the six followers with different initial position states.

6. Conclusion

For the purpose of realizing time-varying formation tracking without the velocity measurements of the leader for the second-order multi-agent systems with unknown uncertainties, this paper has constructed an observer-based fixed-time adaptive formation control scheme. A novel FTCLSO is proposed to guarantee that each follower can obtain the estimates of the leader's states in fixed time with no need for the velocity measurements. By means of utilizing RBFNNs, the model uncertainties are well compensated. The fixed-time convergence of the formation tracking error is proved by Lyapunov approach, and the simulation results verify the effectiveness of the developed control scheme in this paper. In the future, we will further try our best to achieve the fixed-time convergence to the origin of the formation tracking errors under non-smooth backstepping technique and to avoid singularity problem in the meantime. Besides, we will try to extend the obtained results to much more complicated cases, where the followers need to start the formation task when the leader is moving.

CRediT authorship contribution statement

Tianyi Xiong: Conceptualization, Methodology, Software, Formal analysis, Writing - original draft. **Zhou Gu:** Supervision, Writing - review & editing.

Declaration of Competing Interest

The authors declare that they have no known competing financial interests or personal relationships that could have appeared to influence the work reported in this paper.

Acknowledgment

This work is supported by the National Natural Science Foundation of China (Grant No. 61473156).

References

[1] Y. Wang, L. Cheng, Z. Hou, J. Yu, M. Tan, Optimal formation of multirobot systems based on a recurrent neural network, IEEE Trans. Neural Networks Learn. Sys. 27 (2) (2016) 322–333.
[2] X. Dong, Y. Zhou, Z. Ren, Y. Zhong, Time-varying formation control for unmanned aerial vehicles with switching interaction topologies, Control Eng. Pract. 46 (2016) 26–36.
[3] A.K. Das, R. Fierro, V. Kumar, J. Ostrowski, J. Spletzer, C. Taylor, A vision-based formation control framework, IEEE Trans. Rob. Autom. 18 (5) (2012) 813–825.
[4] M.A. Lewis, K. Tan, High precision formation control of mobile robots using virtual structures, Auton. Robots 4 (4) (1997) 387–403.
[5] T. Balch, R.C. Arkin, Behavior-based formation control for multirobot teams, IEEE Trans. Rob. Autom. 14 (6) (1998) 926–939.
[6] T. Xiong, Z. Pu, J. Yi, Time-varying formation finite-time tracking control for multi-uav systems under jointly connected topologies, Int. J. Intell. Comp. Cybern. 10 (4) (2017) 478–490.
[7] W. Ren, Consensus strategies for cooperative control of vehicle formations, IET Control Theory Appl. 1 (2) (2007) 505–512.
[8] F. Xiao, L. Wang, J. Chen, Y. Gao, Finite-time formation control for multi-agent systems, Automatica 45 (11) (2009) 2605–2611.
[9] R. Wang, X. Dong, Q. Li, Z. Ren, Distributed time-varying formation control for multiagent systems with directed topology using an adaptive output-feedback approach, IEEE Trans. Ind. Inf. 15 (8) (2019) 4676–4685.
[10] R. Wang, X. Dong, Q. Li, Z. Ren, Distributed time-varying output formation control for general linear multiagent systems with directed topology, IEEE Trans. Control Netw. Syst. 6 (2) (2019) 609–620.
[11] X. Dong, G. Hu, Time-varying formation control for general linear multi-agent systems with switching directed topologies, Automatica 73 (2016) 47–55.
[12] X. Dong, Y. Zhou, Z. Ren, Y. Zhong, Time-varying formation tracking for second-order multi-agent systems subjected to switching topologies with application to quadrotor formation flying, IEEE Trans. Ind. Electron. 64 (6) (2017) 5014–5024.
[13] E. Tian, Z. Wang, L. Zou, D. Yue, Chance-constrained H_∞ control for a class of time-varying systems with stochastic nonlinearities: The finite-horizon case, Automatica 107 (2019) 296–305.
[14] A. Karimoddini, H. Lin, B.M. Chen, T.H. Lee, Hybrid three-dimensional formation control for unmanned helicopters, Automatica 49 (2) (2013) 424–433.
[15] Z. Zuo, Q. Han, B. Ning, X. Ge, X. Zhang, An overview of recent advances in fixed-time cooperative control of multiagent systems, IEEE Trans. Ind. Inf. 14 (6) (2018), 2322–2234.
[16] A. Polyakov, Nonlinear feedback design for fixed-time stabilization of linear control systems, IEEE Trans. Autom. Control 57 (8) (2012) 2106–2110.
[17] Z. Zuo, L. Tie, A new class of finite-time nonlinear consensus protocols for multi-agent systems, Int. J. Control 87 (2) (2014) 363–370.
[18] D. Zhang, G. Duan, Distributed fixed-time consensus tracking for high-order uncertain non-linear multi-agent systems with switching topologies, IET Control Theory Appl. 13 (11) (2019) 1761–1772.
[19] Z. Zuo, L. Tie, Distributed robust finite-time nonlinear consensus protocols for multi-agent systems, Int. J. Syst. Sci. 47 (6) (2016) 1366–1375.
[20] Z. Zuo, Nonsingular fixed-time consensus tracking for second-order multi-agent networks, Automatica 54 (2015) 305–309.
[21] J. Ni, Y. Tang, P. Shi, A new fixed-time consensus tracking approach for second-order multiagent systems under directed communication topology, IEEE Trans. Syst. Man Cybern. Syst. to be published. doi:10.1109/TSMC.2019.2915562.
[22] Z. Zuo, B. Tian, M. Defoort, Z. Ding, Fixed-time consensus tracking for multiagent systems with high-order integrator dynamics, IEEE Trans. Autom. Control 63 (2) (2018) 563–570.
[23] X. Chu, Z. Peng, G. Wen, A. Rahmani, Distributed fixed-time formation tracking of multi-robot systems with nonholonomic constraints, Neurocomputing 313 (2018) 167–174.
[24] Z. Gao, G. Guo, Fixed-time leader-follower formation control of autonomous underwater vehicles with event-triggered intermittent communications, IEEE Access 6 (2018) 27902–27911.
[25] E. Tian, C. Peng, Memory-based event-triggering H_∞ load frequency control for power systems under deception attacks, IEEE Trans. on Cybern. to be published. doi:10.1109/TCYB.2020.2972384.
[26] X. Liang, H. Wang, Y. Liu, W. Chen, T. Liu, Formation control of nonholonomic mobile robots without position and velocity measurements, IEEE Trans. Rob. 34 (2) (2018) 434–446.
[27] T. Sun, F. Liu, H. Pei, Y. He, Observer-based adaptive leader-following formation control for non-holonomic mobile robots, IET Control Theory Appl. 6 (18) (2012) 2835–2841.
[28] J. Fu, J. Wang, Fixed-time coordinated tracking for second-order multi-agent systems with bounded input uncertainties, Syst. Control Lett. 93 (2016) 1–12.
[29] X. Wu, S. Wang, M. Xing, Observer-based leader-following formation control for multi-robot with obstacle avoidance, IEEE Access 7 (2019) 14791–14798.
[30] Z. Zuo, M. Defoort, B. Tian, Z. Ding, Distributed consensus observer for multi-agent systems with high-order integrator dynamics, IEEE Trans. Autom. Control to be published. doi:10.1109/TAC.2019.2936555.
[31] X. Liu, S.S. Ge, C. Goh, Neural-network-based switching formation tracking control of multiagents with uncertainties in constrained space, IEEE Trans. Syst. Man Cybern. Syst. 49 (5) (2019) 1006–1015.
[32] L. Zhao, Y. Jia, Neural-network-based distributed adaptive attitude synchronization control of spacecraft formation under modified fast terminal sliding mode, Neurocomputing 171 (C) (2016) 230–241.
[33] Y. Zhang, J. Sun, H. Liang, H. Li, Event-triggered adaptive tracking control for multiagent systems with unknown disturbances, IEEE Trans. on Cybern. to be published. doi:10.1109/TCYB.2018.2869084.
[34] J. Qin, G. Zhang, W. Zheng, Y. Kang, Neural network-based adaptive consensus control for a class of nonaffine nonlinear multiagent systems with actuator faults, IEEE Trans. Neural Networks Learn. Sys. 30 (12) (2019) 3633–3644.
[35] D. Ba, Y. Li, S. Tong, Fixed-time adaptive neural tracking control for a class of uncertain nonstrict nonlinear systems, Neurocomputing 363 (2019) 273–280.
[36] J. Liu, Y. Yu, Q. Wang, C. Sun, Fixed-time event-triggered consensus control for multi-agent systems with nonlinear uncertainties, Neurocomputing 260 (2017) 497–504.
[37] Y. Shang, Fixed-time group consensus for multi-agent systems with non-linear dynamics and uncertainties, IET Control Theory Appl. 12 (3) (2018) 395–404.
[38] T. Chen, S. Peng, Z. Zhang, Finite-time and fixed-time consensus of nonlinear stochastic multi-agent systems with rous and rons via impulsive control, IET Control Theory Appl. 7 (2019) 136630–136640.
[39] D. Swaroop, J. k. Hedrick, P.P. Yip, J.C. Gerdes, Dynamic surface control for a class of nonlinear systems, IEEE Trans. Autom. Control 45 (10) (2000) 1893–1899.
[40] X. Shi, J. Lu, Z. Li, S. Xu, Robust adaptive distributed dynamic surface consensus tracking control for nonlinear multi-agent systems with dynamic uncertainties, J. Franklin Inst. 353 (17) (2016) 785–4802.
[41] C. Xi, J. Dong, Adaptive reliable guaranteed performance control of uncertain nonlinear systems by using exponent-dependent barrier lyapunov function, Int. J. Robust Nonlinear Control 29 (4) (2019) 1051–1062.
[42] M. Ge, Z. Guan, C. Yang, Y. Wang, Time-varying formation tracking of multiple manipulators via distributed finite-time control, Neurocomputing 202 (2016) 20–26.
[43] B. Tian, H. Lu, Z. Zuo, W. Yang, Fixed-time leader-follower output feedback consensus for second-order multiagent systems, IEEE Trans. Cybern. 49 (4) (2019) 1545–1550.
[44] J. Ni, P. Shi, Adaptive neural network fixed-time leader–follower consensus for multiagent systems with constraints and disturbances, IEEE Trans. on Cybern. to be published. doi:10.1109/TCYB.2020.2967995.
[45] B. Jiang, Q. Hu, M.I. Friswell, Fixed-time attitude control for rigid spacecraft with actuator saturation and faults, IEEE Trans. Control Syst. Technol. 24 (5) (2016) 1892–1898.
[46] L. Cheng, Z. Hou, M. Tan, Y. Lin, W. Zhang, Neural-network-based adaptive leader-following control for multiagent systems with uncertainties, IEEE Trans. Neural Networks 21 (8) (2010) 1351–1358.
[47] X. Wang, S. Li, P. Shi, Distributed finite-time containment control for double-integrator multiagent systems, IEEE Trans. Cybern. 44 (9) (2014) 1518–1528.
[48] J. Mao, H.R. Karimi, Z. Xiang, Observer-based adaptive consensus for a class of nonlinear multiagent systems, IEEE Trans. Syst. Man Cybern. Syst. 49 (9) (2019) 1893–1900.
[49] M. Basin, C.B. Panathula, Y. Shtessel, Multivariable continuous fixed-time second- order sliding mode control: design and convergence time estimation, IET Control Theory Appl. 11 (8) (2017) 1104–1111.
[50] H. Zhang, F.L. Lewis, Adaptive cooperative tracking control of higher-order nonlinear systems with unknown dynamics, Automatica 48 (7) (2012) 1432–1439.
[51] J. Sun, Z. Pu, J. Yi, Z. Liu, Fixed-time control with uncertainty and measurement noise suppression for hypersonic vehicles via augmented sliding mode observers, IEEE Trans. Ind. Inf. 16 (2) (2020) 1192–1203.
[52] J. Sun, J. Yi, Z. Pu, X. Tan, Fixed-time sliding mode disturbance observer-based nonsmooth backstepping control for hypersonic vehicles, IEEE Trans. Syst. Man Cybern. Syst. to be published. doi:10.1109/TSMC.2018.2847706.
[53] J. Li, Y. Yang, C. Hua, X. Guan, Fixed-time backstepping control design for high-order strict-feedback non-linear systems via terminal sliding mode, IET Control Theory Appl. 11 (8) (2017) 1184–1193.
[54] L. Chen, C. Li, Y. Sun, G. Ma, Distributed finite-time tracking control for multiple uncertain euler–lagrange systems with input saturations and error constraints, IET Control Theory Appl. 13 (1) (2019) 123–133.
[55] W. Fu, J. Qin, Y. Shi, W. Zheng, Y. Kang, Resilient consensus of discrete-time complex cyber-physical networks under deception attacks, IEEE Trans. Ind. Inf. 16 (7) (2020) 4868–4877.

Tianyi Xiong received the Ph.D degree from Institute of Automation, Chinese Academy of Sciences in 2019 and the B.S. and M.S. degrees from Harbin Institute of Technology, in 2014 and 2016, respectively. She is currently a postdoctoral researcher with Nanjing Forestry University, Nanjing, China. Her current research interests include formation control, fixed-time control and network control systems.

Zhou Gu received the B.S. degree from North China Electric Power University, Beijing, China, in 1997 and the M.S. and Ph.D. degrees in control science and engineering from Nanjing University of Aeronautics and Astronautics, Nanjing, China, in 2007 and 2010, respectively. From September 1996 to January 2013, he was with the School of Power engineering, Nanjing Normal University as an associate professor. He was a visiting scholar with Central Queensland University, Rockhampton, Queensland, Australia and The University of Manchester, Manchester, U.K. He is currently a Professor with Nanjing Forestry University, Nanjing, China. His current research interests include networked control systems, time-delay systems, reliable control and their applications.